Bioinspired Scaffold Induced Regeneration of Neural Tissue

Esra Altun, Mehmet O. Aydogdu, Sine O. Togay, Ahmet Z. Sengil, Nazmi Ekren, Merve E. Haskoylu, Ebru T. Oner, Nese A. Altuncu, Gurkan Ozturk, Maryam Crabbe-Mann, Jubair Ahmed, Oguzhan Gunduz, Mohan Edirisinghe

PII: S0014-3057(18)32476-5
DOI: https://doi.org/10.1016/j.eurpolymj.2019.02.008
Reference: EPJ 8862

To appear in: *European Polymer Journal*

Received Date: 17 December 2018
Revised Date: 1 February 2019
Accepted Date: 5 February 2019

Please cite this article as: Altun, E., Aydogdu, M.O., Togay, S.O., Sengil, A.Z., Ekren, N., Haskoylu, M.E., Oner, E.T., Altuncu, N.A., Ozturk, G., Crabbe-Mann, M., Ahmed, J., Gunduz, O., Edirisinghe, M., Bioinspired Scaffold Induced Regeneration of Neural Tissue, *European Polymer Journal* (2019), doi: https://doi.org/10.1016/j.eurpolymj.2019.02.008

Bioinspired Scaffold Induced Regeneration of Neural Tissue

Esra Altun[a], Mehmet O. Aydogdu[a], Sine O. Togay[b], Ahmet Z. Sengil[c], Nazmi Ekren[a,d], Merve E. Haskoylu[e], Ebru T. Oner[e], Nese A. Altuncu[f], Gurkan Ozturk[f], Maryam Crabbe-Mann[g], Jubair Ahmed[g], Oguzhan Gunduz[a,h] and Mohan Edirisinghe[g]*

[a]Center for Nanotechnology & Biomaterials Research, Department of Metallurgical and Materials Engineering, Faculty of Technology, Marmara University, Goztepe Campus, 34722 Istanbul, Turkey

[b]Department of Food Engineering, Faculty of Agriculture, Uludag University, Gorukle Campus 16059 Bursa, Turkey

[c]Department of Medical Microbiology, School of Medicine, Medipol University, Beykoz 34810 Istanbul, Turkey

[d]Department of Electrical-Electronics Engineering, Faculty of Technology, Marmara University, Goztepe Campus 34722 Istanbul, Turkey

[e]IBSB, Department of Bioengineering, Faculty of Engineering, Marmara University, Goztepe Campus 34722 Istanbul, Turkey

[f]Regenerative and Restorative Medicine Research Center (REMER), Department of Physiology, International School of Medicine, Istanbul Medipol University, Beykoz 34810 Istanbul, Turkey

[g]Department of Mechanical Engineering, University College London, Torrington Place, WC1E 7JE, London, UK

[h]Department of Metallurgical and Materials Engineering, Faculty of Technology, Marmara University, Goztepe Campus 34722 Istanbul, Turkey

ABSTRACT

In the last decade, nerve tissue engineering has attracted much attention due to the incapability of self-regeneration. Nerve tissue regeneration is mainly based on scaffold induced nanofibrous structures using both bio and synthetic polymers. The produced nanofibrous scaffolds have to be similar to the natural extracellular matrix and should provide an appropriate environment for cells to attach onto. Nanofibrous scaffolds can support or regenerate cells of tissue. Electrospinning is an ideal method for producing the nanofibrous scaffolds. In this study, Bacterial cellulose (BC)/ Poly (ε-caprolactone) (PCL) blend nanofibrous scaffolds were successfully prepared by electrospinning for nerve tissue induced repair. The produced nanofibrous scaffolds contain well defined interconnected nanofiber networks with hollow micro/nanobeads. Firstly, *in-vitro* biocompatibilities of nanofibrous scaffolds were tested with L2929 murine fibroblasts and improved cell adhesion and proliferation was observed with polymer blends compared with PCL only. The primary cell culture was performed with dorsal root ganglia (DRG) cells on nanofibrous samples and the samples were found suitable for enhancing neural growth and neurite outgrowth. Based on these results, the BC/PCL (50:50 wt. %) nanofibrous scaffolds exhibited nerve-like branching and are excellent candidate for potential biomimetic applications in nerve tissue engineering regeneration.

Keywords: Bacterial cellulose; polycaprolactone; electrospinning; nerve regeneration; biomimetic

1. Introduction

Tissue engineering provides a promising approach for new medical therapy, as an alternative to conventional transplantation methods using bio- or synthetic polymers. Immunological problems and infectious diseases caused by traditional surgical procedures [1] can be avoided by tissue engineering with biopolymers with or without living cells [2]. Nerve tissue regeneration is a valuable remedy making a crucial impact on the quality of human health maintenance. Existing tissue engineering approaches focus on evolving an alternative route for nerve tissue regeneration using polymeric nanofibrous scaffolds and striving to find suitable biomaterials for this [3]. Utilizing the polymeric nanofibrous scaffolds for nerve tissue engineering require the use of constructs which are biodegradable, biocompatible and have high porosity with interconnected pores, and large surface area [4]. Recently, biomimetic alternatives have been developed to imitate natural tissues for use in the rehabilitation of damaged tissues such as skin, bone, dura mater, sciatic nerve, articular cartilage, and tendon in order to enhance functional outcomes [5,6]. Neural tissue engineering includes combination of three-dimensional (3D) scaffolds and many nerve cells to create a biomimetic implantable replacement [7-9].

Electrospinning is an established technique for manufacturing nanofibrous scaffolds, where production of batch quantities of fibers with diameters ranging from several micrometers down to fews of nanometers can be achieved easily with many polymers [10-12]. Both bio- and synthetic polymers can be used as scaffolds to improve cell adhesion, maintenance of differentiated cell function without blocking proliferation, pattern to stimulate and regulate the growth of cells and help in the function of extracellular matrix (ECM) [13,14].

Electrospun neural nanofibrous scaffolds should be biodegradable and have diversity of using natural and synthetic biomaterials such as collagen, poly (ε-caprolactone) (PCL), poly-L-lactic acid (PLLA), polyglycolic acid (PGA), polyurethane (PU), and poly(organo)phosphazenes, which have been discovered as potential biomaterial candidates for neural renewal [15,16]. Hollow micro and nanobeads with nanoscaled wall thickness generates particular interest due to their potential for encapsulation of large quantities of guest molecules inside their empty core space [17]. These

materials could be useful in a multitude of different applications, such as drug release carriers and controlled release systems [18].

Polymer blending is a widely used method for procuring new, enticing biocomposites in tissue engineering applications [19]. PCL is a frequently preferred synthetic biodegradable polyester due to its thermal stability, compatibility, and biological composition [20]. Unlike most polymers, PCL is extremely reliable while evolving the scaffold structure [21]. Electrospun PCL nanofibers matches the individuality of ECM in the living tissues; however, having low hydrophilicity causes limitations in their capability of cell adhesion, migration, proliferation, and discrimination [22]. Previous work documented that PCL ducts are suitable for the survival and differentiation of diverse neural cells with a low risk of rejection [23]. Bacterial cellulose (BC) is generally water insoluble, flexible, biodegradable, elastic polymer with high tensile strength. It has unique physical and mechanical properties, such as crystallinity, biocompatibility, and high permeability. All of these special features makes BC useful for tissue engineering applications [24]. Also, its biocompatibility, hydrophilicity, and non-toxicity makes it a potential candidate for a wide range of applications in various fields, especially in biomedical engineering and biotechnology [25] compared with other biodegradable polymers like collagen, chitosan, and gelatine, BC shows enhanced mechanical properties, which are needed for scaffolds in tissue engineering applications [26]. Its high porosity and surface area allows the potential for entry and release of antimicrobial agents, medicines, and other biofunctional materials [27]. BC shares common features with extracellular matrix components. Kramer and co-workers [28] classified BC as a “collagen-like” material. But, BC has the added benefit of immunologic nonreactivity compared with collagen [29].

Peripheral nervous system (PNS) damages may cause malfunction of sensory and/or motor features, leading to poor recovery of function [30]. Therefore, treatments of functional disorders affecting the PNS are limited when injury creates a large gap (>3 cm) in the peripheral nerves and those large gaps can delay axon regrowth and compromise a time-effective reconnection of the nerve stumps [31,32]. However, neural tissue engineering can mimic for nerve regeneration through the scaffold and the function can be recovered for large gaps as stated in previous studies [33-35]. In this case,

using a BC/PCL nanofibrous scaffold can provide scaffold-induced repair by providing an optimal microenvironment for cell proliferation, migration, differentiation and improved the cell adhesion due to characteristics of component materials of the blend while benefiting the high surface/volume ratio of the nanofibrous scaffold production mechanism.

This study aims to fabricate and explore the detailed properties of BC/PCL (50:50 wt.%) nanofibrous scaffolds for enhancing of PNS neural tissue regeneration and neurite outgrowth prepared using electrospinning.

2. Materials and Methods

2.1. Materials

Poly (ε-caprolactane) (PCL, MW 80000 g/mol), Chloroform ($CHCl_3$), Dimethyleformamide (DMF) and Tetrahydrofuran (THF) were supplied by Sigma-Aldrich (St. Louis, MO, USA). The bacterial cellulose (BC) was provided by the Department of Medical Microbiology, Medipol University (Istanbul, Turkey). All reagents were analytical grade and were used as received.

2.2. Bacterial cellulose preparation

Gluconacetobacter xylinus ATCC 700178 strain (**Figure 1A(i)**) was cultured in 10 ml of Hestrin-Schramm (HS) medium consist of (2 % (w/v) D-glucose, 0.5% (w/v) peptone, 0.5 % (w/v) yeast extract, 0.27 % (w/v) Na_2HPO_4, 0.115 % (w/v) citric acid) and incubated at 30°C under shaker conditions (150 rpm) for 3-7 days. The activated culture was then transferred into 600 ml HS medium and production of bacterial cellulose was maintained for 7 days in the static conditions at 30°C. Appearance of a white film-like layer was observed (**Figure 1A(ii)**). This layer was removed from growth medium and purified by boiling with 1.0 % NaOH for 2 hours and this process was repeated again for further purification. Then the resultant solution was treated with 1.5 % acetic acid for 30 minutes and finally thoroughly washed with water until BC pellicles became neutral and subsequently these were immersed in distilled water prior to use [36].

2.3. Preparation of solutions

5 % (w/w) PCL was dissolved in $CHCl_3$/DMF (50:50 wt. %) while stirring in a conical flask at 50°C for 1.5 hours. BC was then dissolved in a conical flask at a concentration of 5 % (w/w) in

DMF/THF (50:50 wt. %) (**Figure 1A(iii)**) and the dissolution process was accelerated by ultrasonic agitation (CEIA, CP102, Italy) (**Figure 1A(iv)**). This was carried out for 5 hours at 70 % of the intensity at 70°C over 15 days. Dissolution steps were captured by optical microscopy (The Olympus® Color View Microscope, USA). **Figure 1B** shows the dissolution process of BC; **Figure 1B(i)** demonstrates Days 1-3 with no disintegration. **Figure 1B(ii)** shows the slight softening observed on the surface and edges of BC in days 4-6. **Figure 1B(iii)** illustrates days 7-9 with the decomposition of BC particles. **Figure 1B(iv)** exhibits further results of dissolution at days 10-12, where disintegration of whisker like structures of BC was noticed. **Figure 1B(v)** and **(vi)** show the final condition of BC dissolved in the DMF/THF solution from day 1 to day 15. As defined in an earlier study by Sacui et al. [37] who prepared BC/hydrochloric acid and BC/sulfiric acid solutions by hydrolysis, rodlike nanocrystals and most likely hydrolysis-resistant particles in the tens to hundreds of micrometer scale were prepared. In another study, Olsson and co-workers [38] prepared BC microfibril-poly(methyl methacrylate) nanocomposite in DMF:THF (50:50 vol. %) electrospinning technique, and this was achieved by stirring of the solutions. Yet another study by Paximada et al. [39] prepared BC consisting of an entangled fibril network by using an ultrasonic homogenizer, here the fibrils where of width 110 nm to 60 nm. Unlike these, in the present study, BC whiskers and particles of micrometer to nanometer size was obtained in the DMF/THF (50:50 wt. %) solution and the final suspension was used without further treatment.

After the dissolution process BC and PCL solutions were blended at a concentration of 50:50 wt. %. The blend solution was stirred with a magnetic stirrer for 2 hours prior the electrospinning at ambient temperature (23°C).

2.4. Fabrication of PCL and BC/PCL nanofibrous scaffolds

The electrospinning device (NS24, Inovenso ltd., Istanbul, Turkey) consists of a grounded high voltage power supply (**Figure 1C(i)**, Matsusada Precision Inc., Kyoto, Japan), which generates positive DC applied voltages up to 60 kV, a high precision syringe pump (**Figure 1C(ii)**, World Precision Instruments, Florida, USA) to control the flow rate of the blend solution to the nozzle, a single stainless steel electrospinning nozzle provided by Inovenso Ltd. (**Figure 1C(iii)**, Istanbul, Turkey), and a high speed rotating drum up to 2000 rpm (**Figure 1C(iv)**), which is covered with non-stick paper to collect the fibers. **Figure 1C(v)** shows close up image of the nozzle in action during the experimental process. Outer and inner orifice diameters of the stainless steel nozzle were

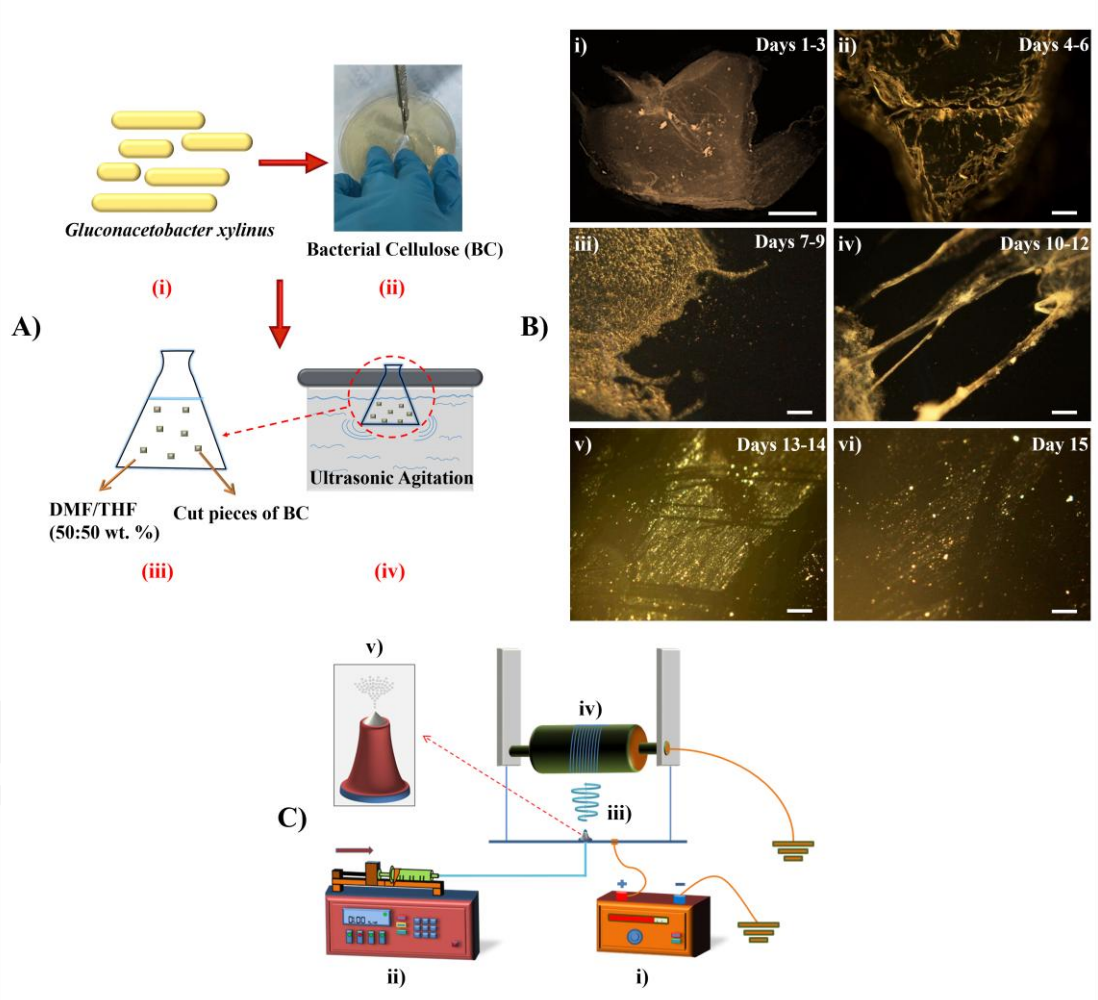

3000 µm and 850 µm, respectively.

Figure 1. Preparation of solutions and nanofibrous scaffolds. **A)** Schematic illustration of BC dissolution process: **(i)** *Gluconacetobacter xylinus* strain used as the source of BC, **(ii)** during

cutting process white and film-like layer of BC mat forms, **(iii)** cut pieces of BC 5 % (w/w) in DMF/THF solution (50:50 wt. %), **(iv)** dissolution of BC with the aid of ultrasound. **B)** Optical images of BC dissolution: **(i)** Days 1-3, **(ii)** Days 4-6, **(iii)** Days 7-9, **(iv)** Days 10-12, **(v)** Days 13-14, **(vi)** and Day 15. Scale bars are 1 mm. **C)** Schematic drawing of electrospinning experimental setup: **(i)** high voltage power supply, **(ii)** high precision syringe pump, **(iii)** stainless steel electrospinning nozzle, **(iv)** high speed rotating drum, **(v)** electrospinning nozzle features.

The nozzle inlet was connected to a plastic sterile syringe (Set Medical Industry and Trade Inc., Istanbul, Turkey) with silicone tubing (Cakir Kimya Ltd., Istanbul, Turkey) and a stainless steel laboratory jack was placed underneath the nozzle and silicone tubing, and it was kept positively charged. Sterile syringe with 10 ml volume capacity was loaded to the syringe pump containing the BC/PCL (50:50 wt. %) blend solution and silicone tubes were used to transfer the blend solutions to the nozzle. For each individual set of experiments, ambient conditions were optimised for temperature (23 to 24^{o}C) and relative humidity (52 to 54 %) using the air conditioning. Voltage was set to 28 kV and the flow rate of the blend solution was fixed at 1 ml/hr. The working distance between the nozzle tip and the high speed rotating drum was set to 130 mm. The grounded electrode was connected to the high speed rotating drum, where the fibrous mats were collected. After 5 hours of electrospinning, ~2.8 g of fibres were collected from the high speed rotating drum and they were left to dry in the oven at 50°C for 24 h. In addition to that, 5 wt. % PCL solution was loaded to sterile syringe as a control group and electrospinning experiments were done as same as the BC/PCL (50:50 wt. %) blend solution.

2.5. Solution properties

Viscosity, density, electrical conductivity and surface tension of the solutions were measured using calibrated equipment. Viscosity of 5 wt. % PCL solution and BC/PCL (50:50 wt. %) solution samples was determined by a Viscometer (Brookfield DV-E, Massachusetts, USA) at 20^{o}C over a 120 s time period at 1000 rpm and 5 samples of each 5 wt. % PCL solution and BC/PCL (50:50 wt. %) solution were tested and the mean value was noted. Electrical conductivity of 5 wt. % PCL

solution and BC/PCL (50:50 wt. %) solution samples were measured using a WTW, Cond 3110 SET1 (Germany) instrument. It was used to obtain at least five stabilized values for each of 5 wt. % PCL and BC/PCL samples. Also, the density of the solutions was measured with a standard 25 ml density bottle. Surface tension of the solutions was measured using a SIGMA 703D tensiometer (Biolin Scientific, UK) by the Wilhelmy's plate method. All the viscosity, density, electrical conductivity and surface tension values are given in **Table 1**.

Table 1. Physical properties of prepared solutions.

SAMPLE NAME	Viscosity (mPa s)	Density (kg/m^3)	Electrical Conductivity (µS/cm)	Surface Tension ($mN\ m^{-1}$)
5 wt. % PCL	65.8 ± 0.2	0.950 ± 0.002	3.9 ± 0.1	29.3 ± 0.8
BC/PCL (50:50 wt. %)	92.1 ± 0.3	1.060 ± 0.010	5.1 ± 0.2	30.0 ± 1.3

2.6. Fiber morphology

The shape, size, surface morphology, and arrangement of fibres in the electrospun 5 wt. % PCL and BC/PCL (50:50 wt. %) nanofibrous scaffolds and the internal structure of the embedded hollow micro/nanobeads were studied by scanning electron microscopy (LYRA3 FEG-SEM, TESCAN, USA). The samples were sputter-coated with a gold layer of approximately 30 nm thickness and FEG-SEM imaging was studied under an accelerating voltage of 10 kV.

2.7. ζ -potential

ζ-potential was measured with a SurPASS™ 3 (Anton Paar GmbH, Graz, Austria) analyser at 25°C. Two samples of BC/PCL (50:50 wt. %) nanofibrous scaffolds were cut to a size of 20 mm x 10 mm, which is ideal for mounting in the adjustable gap cell of the SurPASS™ 3 instrument. The samples

were fixed on sample holders using double-sided adhesive tape and aligned opposite to each other, thereby introducing a gap size of 100 μm. The measuring liquid, an aqueous solution of a 1:1 electrolyte (Potassium chloride, KCl, Sigma-Aldrich, St. Louis, MO, USA), at a reasonable ionic strength (0.001 mol/L), passes the slit channel formed between sample surfaces. A pressure difference applied between both ends of this streaming channel drives the liquid flow and thus the generation of the streaming potential signal. ζ-potential is the measure of charge repulsion or attraction within a structure [40]. This was measured in acidic condition. The measurements were started at the native pH 6 of an aqueous 0.001 mol/L KCl solution and advanced towards the isoelectric point (IEP, i.e., pH where = 0 mV and thus the interfacial charge diminishes). Consequently, the measuring cell with sample was rinsed with MilliQ water and the titration was continued towards higher pH after replacing the KCl solution. The measurements are reported as the mean of at least three prepared samples.

2.8. Fourier-transform infrared spectroscopy (FT-IR)

The interaction between BC and PCL was studied using FT-IR spectroscopy (Shimadzu-IRPrestige-21, Kyoto, Japan) to confirm the presence of BC in the PCL nanofibrous scaffolds. The samples of pure BC, pure PCL and electrospun BC/PCL (50:50 wt. %) nanofibrous scaffold were inserted into the FT-IR spectrometer and 10 scans with a resolution of 4 cm^{-1} in the 4000-600 cm^{-1} region were carried out for each sample.

2.9. Tensile testing

Mechanical properties of the electrospun 5 wt. % PCL and BC/PCL (50:50 wt. %) nanofibrous scaffolds (**Figure 2)** were measured with a universal testing machine (INSTRON 4411, Massachusetts, USA) at 19°C. A digital micrometer (795.1 MEXFL-25, Starrett, USA) was used, and the samples were held between two glass microscope slides. Three nanofibrous scaffold samples were arranged in the form of rectangular shape and loaded to its breaking point at a crosshead speed of 5 mm/min. The thickness of three samples were measured and the tensile strength values are given alongside the respective micrographs in **Figure 2**.

2.10. Biocompatibility

To determine the overall biocompatibility of the 5 wt. % PCL and BC/PCL (50:50 wt. %) nanofibrous scaffolds, proliferation and cell viability assays were performed with L929 (Murine fibroblast cell line) (ATCC-CCL-1) *in-vitro*. To estimate the number of viable cells, cell proliferation reagent WST-1 (4-[3-(4-iodophenyl)-2-(4-nitrophenyl)-2H-5-tetrazolio]-1, 3-benzenedisulfonate) (Roche Diagnostics, Germany) was used. Nanofibrous scaffolds were sterilized with UV on both sides (30 minutes each), with 70 % ethanol. After sterilization, samples were rinsed in 1 % Penicillin-Streptomycin (PAN Biotech, Germany) in PBS (Phosphate Buffer Solution, Amresco, USA) solution for 2 hours, and saturated with DMEM (PAN Biotech, Germany) complete medium for 1 hour. Then nanofibrous scaffolds were placed into 24-well culture plates and were seeded with 2×10^4 cells per well. Seeded cells were incubated with nanofibrous scaffolds for 24, 48 and 72 hours at 37°C in humidified air containing 5 % CO_2 under sterile conditions. At the end of the incubation period, WST-1 reagent was added directly to culture wells and incubated for another 2 hours. Absorbance values were measured with a Glomax Multi + Microplate Multimode Reader (Promega, USA) at 450 nm. As a control group, cells incubated without nanofibrous scaffolds were also used. The control group was considered as 100 % viable.

Growth of L929 murine fibroblast cells on nanofibrous scaffolds was visualized with a fluorescence microscope (Leica DM LB2, Leica Microsystems, Wetzlar, Germany). For this, nanofibrous scaffolds were fixed with 4 % paraformaldehyde in PBS solution. After the incubation period, nuclei of the cells were stained with DAPI (4',6-diamidino-2-phenylindole) (Applichem, Germany) fluorescent dye. After staining, excess dye was washed and samples were dehydrated by rinsing with increasing ethanol concentrations (70 %, 80 %, 96 % and 100 %) and then fluorescent microscopy images were taken.

2.11. Primary neuronal cell culture

Dorsal root ganglia (DRG) sensory neurones were chosen to support axon regeneration into the peripheral nervous system (PNS). The isolation of DRG sensory neurones was based on a protocol validated by Demir et al. [41]. Young adult (6–8 weeks) mice were anaesthetized by an I.P. injection of ketamin (100 mg/kg, Ketalar, Pfizer), sacrificed by cervical transection and 35–40

DRGs were quickly and aseptically removed under a stereomicroscope. After trimming all attached nerves in RPMI 1640 medium (Sigma, MO, USA), they were transferred to Neurobasal A medium supplemented with 2 % B27 (NBA-B27) (Invitrogen, CA, USA) containing 2 mM Glutamax-I (Invitrogen MO, USA), 100 units of Penicillin, 100 mg Streptomycin and 250 ng amphotericin B per ml (Sigma, MO, USA) and 100 U/ml collagenase (Sigma, MO, USA). After 50 min of incubation (37°C, 5 % CO_2) DRGs were washed three times in Hank's buffered salt solution (Sigma, MO, USA) and they were subjected to further enzymatic digestion with trypsin (1 mg/ml) in NBA-B27 for 15 min in the incubator. Then, DRGs were triturated for about 15 min by gently and repeatedly pipetting through the tips of narrowing bores (from 2 mm diameter down) and finally through a 26-gauge injector needle. DNAse (50 mg/ml) (Sigma, MO, USA) was added to the cell suspension obtained, which was then returned to the incubator and kept there for another 30 min, this time on a custom made agitator horizontally vibrating at 50 Hz. After this, the suspension was spun at 1000 rpm for 3 min, the supernatant was discarded and the pellet was resuspended in NBA-B27 containing 10 % fetal calf serum (Sigma, MO, USA) and 700 mg/ml trypsin inhibitor (Sigma, MO, USA) to neutralize the activity of the residual digestive enzymes. The cell suspension was then carefully pipetted on top of a three-layer percol (Sigma, MO, USA) gradient (60 %, 35 % and 10 % from bottom to top) prepared with NBA-B27 in a plastic tube and spun at 1700 rpm for 20 min in a centrifuge cooled down to 4°C. Neurons were collected from 35 % layer, washed with NBA-B27 and spun once more at 1000 rpm for 3 min; the supernatant was discarded and the pellet was resuspended in NBA-B27.

This final cell suspension was seeded on coverslips, which had been previously covered with poly-l-lysine (1.8 mg/cm^2, 3h at RT) and then laminin (40 ng/mm^2, overnight at 37°C) in control and BC/PCL (50:50 wt. %) nanofibrous scaffold and then laminin (40 ng/mm^2, overnight at 37°C) in other groups. The dishes were left in the incubator for 2 h to let the neurons attach to the bottom, after which they were gently washed to remove unattached cells and remaining debris and finally filled with NBA-B27 and returned to the incubator.

At the 48th hour of incubation, neurons were visualized on a laser scanning confocal microscope (Zeiss LSM 780). Also, neurite lengths were measured using Image J programme.

2.12. Fixation of cells for SEM

Cells were first washed with PBS and fixed with 2.5 % gluteraldehyde. Then, they were washed with distilled water for 3x5 min, after which they were dehydrated through 30, 50, 70, 80, 90, 96, and 100 % alcohol series each lasting 5 min. Then, they were passed through 30 % and 50 % acetone series for 5 min and taken to 100 % acetone. Samples were sputter coated with gold for 60 seconds using a Quorum SC7620 Mini Sputter Coater before imaging.

2.13. Statistical analysis

For statistical analyses, Graph Pad V 5.0 Prism program was used. Mann Whitney U and One-Way ANOVA with post hoc Tukey's tests were used to compare groups. All quantitative triplicate experiments and data were presented as means and 95 % confidence interval (CI). A p-value below 0.05 was considered as statistically significant.

3. Results and discussions

3.1. Scaffold structure, morphology and mechanical properties

BC/PCL (50:50 wt. %) nanofibrous scaffolds, which includes nanosized fibres and embedded hollow micro/nanobeads were produced using the electrospinning method (**Figure 2**). Lin et al. [42] produced beaded polystyrene nanofibres by varying the polymer concentrations and viscosities in different weight ratios of DMF/THF solvent mixtures. Applied voltage, viscosity of the solution, charge density and surface tension of the solution are the factors affecting the bead formation in the electrospinning process [43]. Furthermore, as it is well known, raising the solution viscosity, density and electrical conductivity by increasing polymer concentration provides uniformly beaded fibers [44-46]. In this work, viscosity and electrical conductivity were substantially raised when compared to the 5 wt. % PCL solution (**Table 1**) and these properties can be the reason for forming embedded hollow micro/nanobeads. Since the solution was carrying very fine particles and whiskers of BC, the polymer blend of BC displayed suspension properties which created a fluctuation on the solution properties at the top of the needle which is constantly exposed to

electrical forces to form fibres. We believe that this fluctuation happened due to the presence of BC and its interaction with PCL within the solution causing hollow micro/nanobeads to form. After the micro/nanobeads are formed, charge concentration at the end of the micro/nanobeads exerted a repulsive force on the micro/nanobeads and it caused beads to expand and even triggered beads to split apart and create more micro/nanobead structures [47]. The extension during this period caused an increased surface area on the micro/nanobead structures and possible separations were also induced by the same mechanism, eventually creating hollow micro/nanobead structures consisting of BC and PCL. However, the mechanism of forming the internal hollow structures in the micro/nanobeads during one-step electrospinning method still needs further investigation.

Figure 2A(i) shows FEG-SEM images of the 5 wt. % PCL nanofibrous scaffold at low magnification (500x) and **(ii)** shows the BC/PCL (50:50 wt. %) nanofibrous scaffold at a much higher magnification (9590x), clearly showing the nanofibers and embedded hollow micro/nanobeads. At a higher magnification (63200x), for BC/PCL (50:50 wt. %) nanofibrous scaffold structure contains microbeads and resembles the human neurological system. Diameters of the nanofibers were ~527 nm for 5 wt. % PCL nanofibrous scaffold and were in the range of 70-120 nm for the BC/PCL (50:50 wt. %) nanofibrous scaffold. Embedded hollow micro/nanobeads of BC/PCL (50:50 wt. %) nanofibrous scaffold were 100 nm to 1.6 μm in size, and their internal hollow structure was measured to be 80 nm to 1.2 μm. The shell thickness of a microcapsule (with internal hollow structure) was ~100 nm.

Micro/nanobeads from biopolymers having a hollow structure inside are very much desired for diverse applications due to their exceptional physical and chemical attributes [48], such as utilisation in controlled release of drugs, cell and enzyme transplantation, gene therapy [49]. Structures found in our micrographs are similar to neurons, which are the smallest units of human neurological system and its branching reticulated pattern [50].

Thickness of BC/PCL (50:50 wt. %) nanofibrous scaffold mats were measured ~0.03 mm. Accurate measurement of thickness is one of the key parameters for the evaluation of tensile measurements of nanofibrous scaffolds [51]. The maximum tensile strength of BC/PCL (50:50 wt. %) nanofibrous scaffolds was ~30 MPa and higher than the average tensile strength for 5 wt. % PLC (~14.6 MPa) and those reported in the literature for PCL compositions with other biopolymers [52,53]. An ideal guest scaffold should have extraordinary mechanical strength, which makes the nanofibrous scaffold reported in this study more suitable for neural tissue engineering [54]. Therefore, these results are promising for enhancing the mechanical properties of PCL fibres.

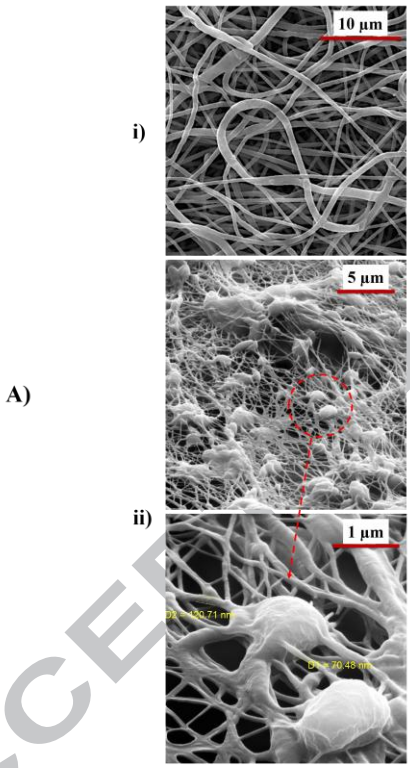

SAMPLES	Thickness Measurement (mm)	Tensile Strength (MPa)
5 wt. % PCL Nanofibrous Scaffold	0.030± 0.008	14.6 ± 2.5
BC/PCL (50:50 wt. %) Nanofibrous Scaffold	0.030 ± 0.002	29.3 ± 3.8

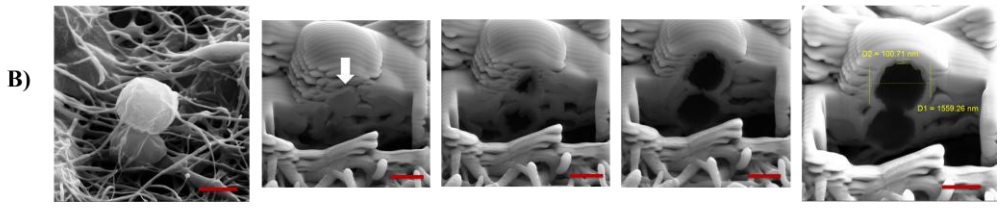

Figure 2. Morphological features and mechanical properties of produced nanofibrous scaffolds. **A)** FEG-SEM images of the 5 wt. % PCL nanofibrous scaffold **(i)-(ii)** and BC/PCL (50:50 wt. %) nanofibrous scaffold with embedded hollow micro/nanobeads and nanofibrous scaffold structure with tensile strength indicated alongside. **B)** FEG-SEM images illustrating the progressive slicing of

an embedded hollow microbead from BC/PCL (50:50 wt. %) nanofibrous scaffold. Overall plan view prior to sectioning, thinning on the surface (indicated by an arrow), emerging hollow structure, thin layer surrounding the microbead and internal diameter and shell thickness of microbead can be seen from right to left. (All the scale bars are 1 μm)

Two microbeads and some nanobeads can be seen in **Figure 2B**. One of the microcapsules was randomly selected for focused ion beam sectioning and progressive slicing. **Figure 2B** revealed that these are hollow structures. Previous studies, have reported fibrous mats with beads [55,56], but in contrast our beads are hollow rather than solid or porous on the surface.

3.2. Characteristics of BC/PCL nanofibrous scaffolds

3.2.1. ζ-potential and charge of nanofibrous scaffolds with FT-IR

The ζ-potential of the BC/PCL (50:50 wt. %) nanofibrous scaffold sample was measured, a reading was taken at 200 Pa pressure. Due to size of the BC/PCL (50:50 wt. %) nanofibers (70-120 nm) the streaming potential was found to be –28 mV (**Figure 3A(i)**). **Figure 3A(ii)** shows the pH dependence of the ζ-potential for the nanofibrous scaffolds and different values of ζ-potential analysis are indicated with circular symbols. The high reproducibility of the ζ-potential at pH 6 indicates that no changes occurred to the nanofibrous scaffold surface after exposure to acidic pH. The isoelectric point (iep) at pH 3.8 is in the pH range expected for BC and PCL [57]. While literature data on the zeta potential available for fibrous material can be underestimated [58], the ζ-potential of BC/PCL nanofibrous scaffolds suggests that BC possesses acidic surface groups (–OH groups) and the orientation of PCL's carbonyl groups causes its low iep and can be attributed to the increase in hydrophobicity of the material.

The interpretation of the FT-IR spectra (**Figure 3B**) indicates peaks at 3340, 2889, 1640 and 1055 cm^{-1} which are associated with pure BC [59]. The peak at 3340 cm^{-1} arises from the stretching of O-H groups. The bands at 2900 and 1640 cm^{-1} originate from the C-H stretching and the O-H deformation. A strong peak at 1055 cm^{-1} is caused by the C–O–C pyranose ring skeletal vibration. With regards to pure PCL powder, stretching modes are assigned to the peaks at 2952 cm^{-1}

(asymmetric CH_2 stretching) and 2870 cm^{-1} (symmetric CH_2 stretching), 1720 cm^{-1} (C=O stretching), 1292 cm^{-1} (basis C-O and C-C stretching in the crystalline phase), 1050 cm^{-1} (asymmetric C-O-C stretching) and 730 cm^{-1} (basis C-C rocking). Regarding the BC/PCL electrospun nanofibrous scaffolds, all spectra include a band at ~1720 cm^{-1} characteristic of the carbonyl stretching mode of the ester groups of PCL [60]. However, the intensity reduction of the peaks at 1292, 1720, 1050, and 730 cm^{-1} does indicate same physical interaction between PCL and BC chains.

Figure 3. ζ-potential and FT-IR characteristics of the nanofibrous scaffolds. **A) (i)** Pressure ramp

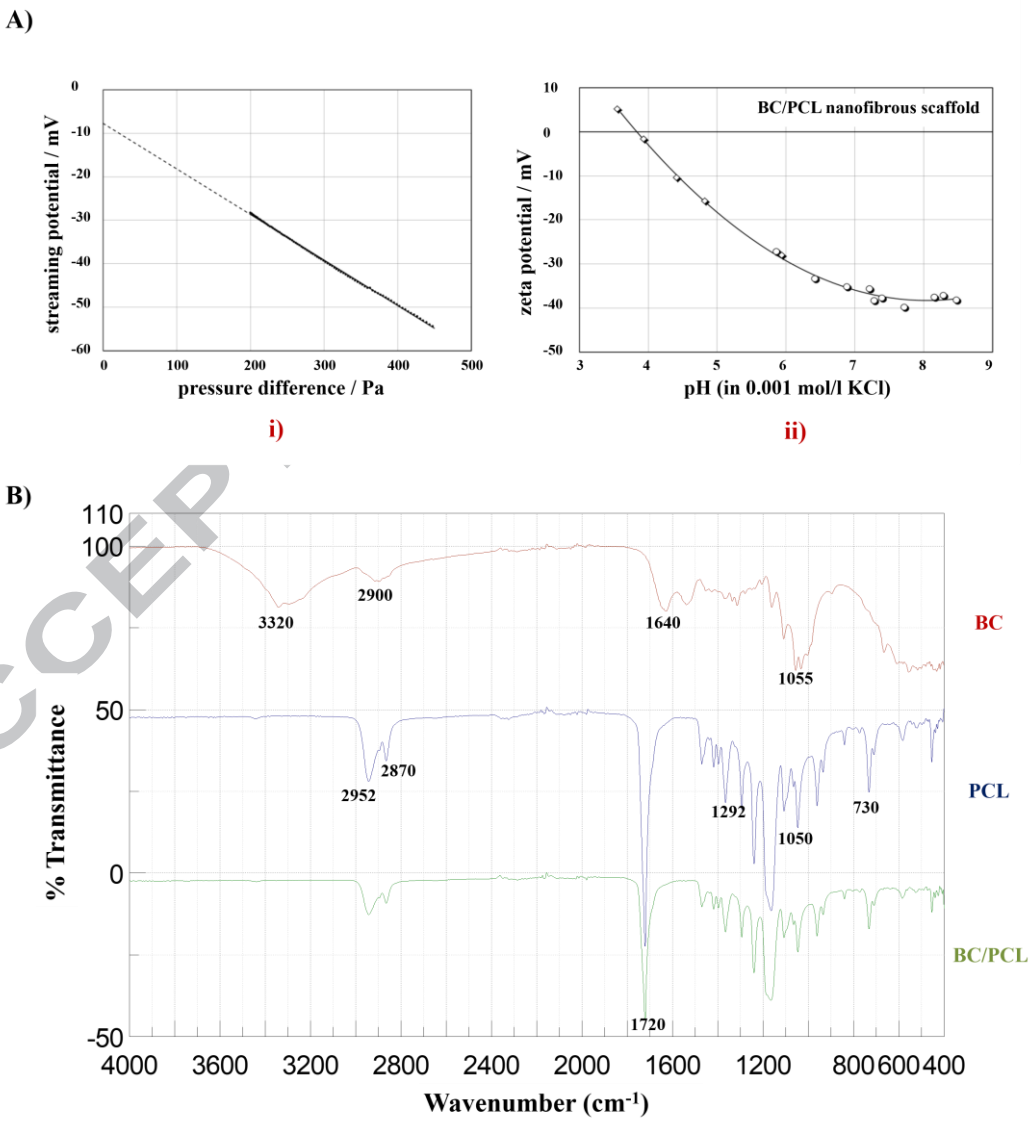

(streaming potential vs differential pressure) for BC/PCL nanofibrous scaffold measured at pH 6,

(ii) pH dependence of ζ-potential for BC/PCL nanofibrous scaffods. **B)** Typical FT-IR spectra of BC/PCL nanofibrous scaffolds.

3.3. *In-vitro* cell viability

Since fibroblast cells play an important role in tissue repair, proliferation and cell viability of L929 murine fibroblast cells on nanofibrous scaffolds were investigated for 24, 48 and 72 hours. Cell behaviour on 5 wt. % PCL and BC/PCL (50:50 wt. %) samples were observed via fluorescent microscopy and images were captured with IM50 in this study. After 24, 48 and 72 hour incubations with cells, DAPI stained cells were analysed. While the viability of the 5 wt. % PCL and BC/PCL (50:50 wt. %) samples were 84 % at the end of 24 h (**Figure 4(A)**), respective viabilities changed to 80 % for 5 wt. % PCL and 83 % for BC/PCL (50:50 wt. %) (**Figure 4(B)**) after 48 h and then to 85 % for 5 wt. % PCL and 93 % for BC/PCL (50:50 wt. %) after 72 h (**Figure 4(C)**). It was clearly shown in the fluorescent images that cells attached on samples and cell population increased with time. Increased cell adhesion on BC/PCL (50:50 wt. %) samples can be explained with properties and similarities of BC with cellular biological environment. It is known that cell attachment is affected by natural extracellular matrix, which has structural components in the nanoscale [61]. Thus, mimicking natural environment for cells when cultured *in-vitro* is highly important. Diameter of fibers may affect cell adhesion on nanofibrous scaffolds but optimum size may differ from one cell type to another [62]. It is known that mesenchymal stem cells grow better on 1 μm diameter fibers than on 500 nm fibers [62]. Sangsanoh et al. [63] investigated viability of Schwann cells on five different polymer materials for 3-5 days. Results showed that viability is increased on 1-4 μm diameter fibers compared to others. According to results of this study, nanofibers diameter of BC/PCL (50:50 wt. %) samples (70-120 nm) have the ability to increase cell viability and differentiation of cells.

Native BC has good biocompatibility with murine fibroblast cells (L929) [64]. Mesenchymal stem cells proliferated on BC and expressed nerve growth factor (Neutrophin) to create a microenvironment that promoted neuronal regeneration [65]. It is known that proliferation and attachment of cells increase when synthetic fibers are blended with biological polymers.

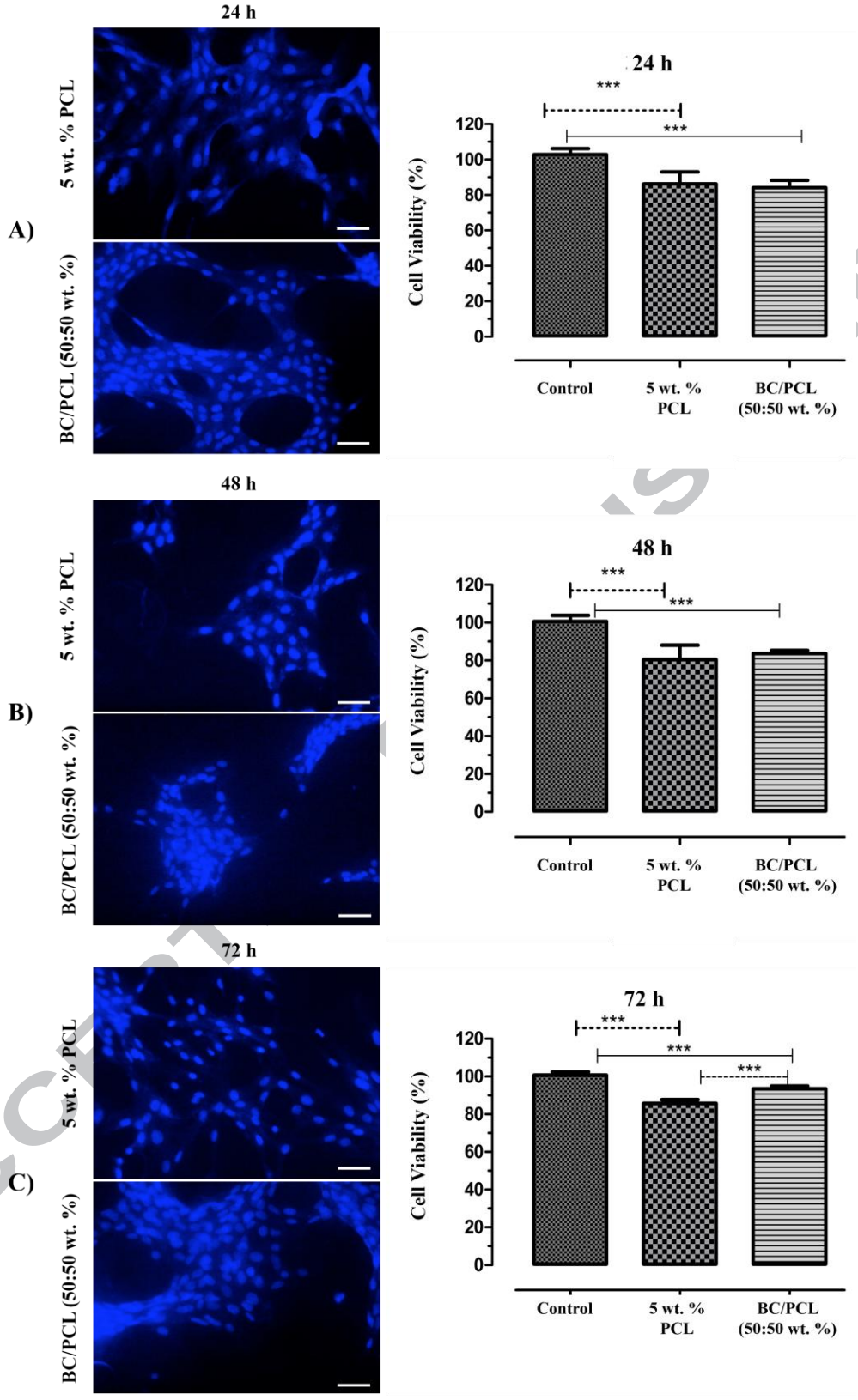

Figure 4. *In-vitro* cell viability and fluorescent microscopy results of nanofibrous scaffolds. L929 murine fibroblast fluorescent microscopy and cell viability results post culture with 5 wt. % PCL and BC/PCL (50:50 wt. %) nanofibrous scaffold for **A)** 24, **B)** 48 and **C)** 72 hours. (P value < 0.05 represented as *** and all the scale bars are 100 μm)

Ghasemi-Mobarakeh et al. [66] studied nerve differentiation on PCL/gelatin blends and concluded that PCL/gelatin enhanced nerve differentiation compared to plain PCL nanofibrous scaffolds. Similarly, Zhang and others [67] investigated biocompatibility of PCL and PCL/collagen nanofibers with primer human fibroblasts and results showed that PCL/collagen blends showed better proliferation than native PCL nanofibers.

From the *in-vitro* cell viability and fluorescent microscopy results, it can be concluded that nanofibrous scaffolds are not cytotoxic. Moreover, time dependent cellular viability increase in BC/PCL (50:50 wt. %) samples shows that these nanofibrous scaffolds are biocompatible. Fluorescent microscopy images also lead to the conclusion that cellular adhesion on BC/PCL samples were more intense than on PCL samples. According to these results it can be concluded that the blend of BC with PCL increased biocompatibility and adhesion of cells.

3.4. Neuronal cultures

BC and BC-based composites have been used as scaffolds for cell seeding. Several studies have confirmed that different cells, such as human embryonic kidney cells (HEK) [68], bone forming osteoblasts (OB) [64], fibroblasts [64], chondrocytes [69], human smooth muscle cells (SMC) [29], SH-SY5Y, N1E-115 and PC12 [70] can grow in the presence of BC. However, its use in primary cell culture is not very common and there is no previous work dealing with BC in primary cell culture with Dorsal root ganglia (DRG) neurons. DRG neurons transfer axonal projections into peripheral tissues, including skin, muscle and visceral organs [71]. Because of that, the use of DRG cells in primary cell culture in this study allows us to see the interaction with BC/PCL (50:50 wt. %) nanofibrous samples.

After 2 hours of culture the DRG sensory neurons attached to the bottom of the culture dish and began growing neurites. The DRG explant system allowed interactions between nanofibers, migrating glia and regenerating neurites *in-vitro*. After 48 h of incubation Laser Scanning Confocal Microscopy and SEM were performed with dissociated DRG sensory neurons **(Figure 5).** The representative Laser Scanning Confocal Microscope and SEM images of DRG cells cultured for 48

hours are shown in **Figure 5A** for control group and BC/PCL (50:50 wt. %) nanofibrous scaffold group. Laser Scanning Confocal Microscope images confirmed that BC/PCL (50:50 wt. %) nanofibrous scaffold can provide a suitable environment for migrating glia and regenerating neurites. In the SEM images of BC/PCL (50:50 wt. %) nanofibrous scaffold group the cell body had a conspicuously bipolar elongated morphology with the outgrowing neurites. Furthermore, both neural elongation and neurite outgrowth follow the same direction of BC/PCL (50:50 wt. %) nanofibrous scaffold as reported in previous studies [72, 73].

Figure 5. Laser Scanning Confocal Microscope and SEM images and axon size measurements of DRG sensory neurons on the BC/PCL nanofibrous scaffold. **A)** Both Laser Scanning Confocal Microscope and SEM images of neurons under cultured conditions and on BC/PCL (50:50 wt. %) nanofibrous scaffold at the end of 48 h of incubation. (Thick and thin arrows point to neuron bodies

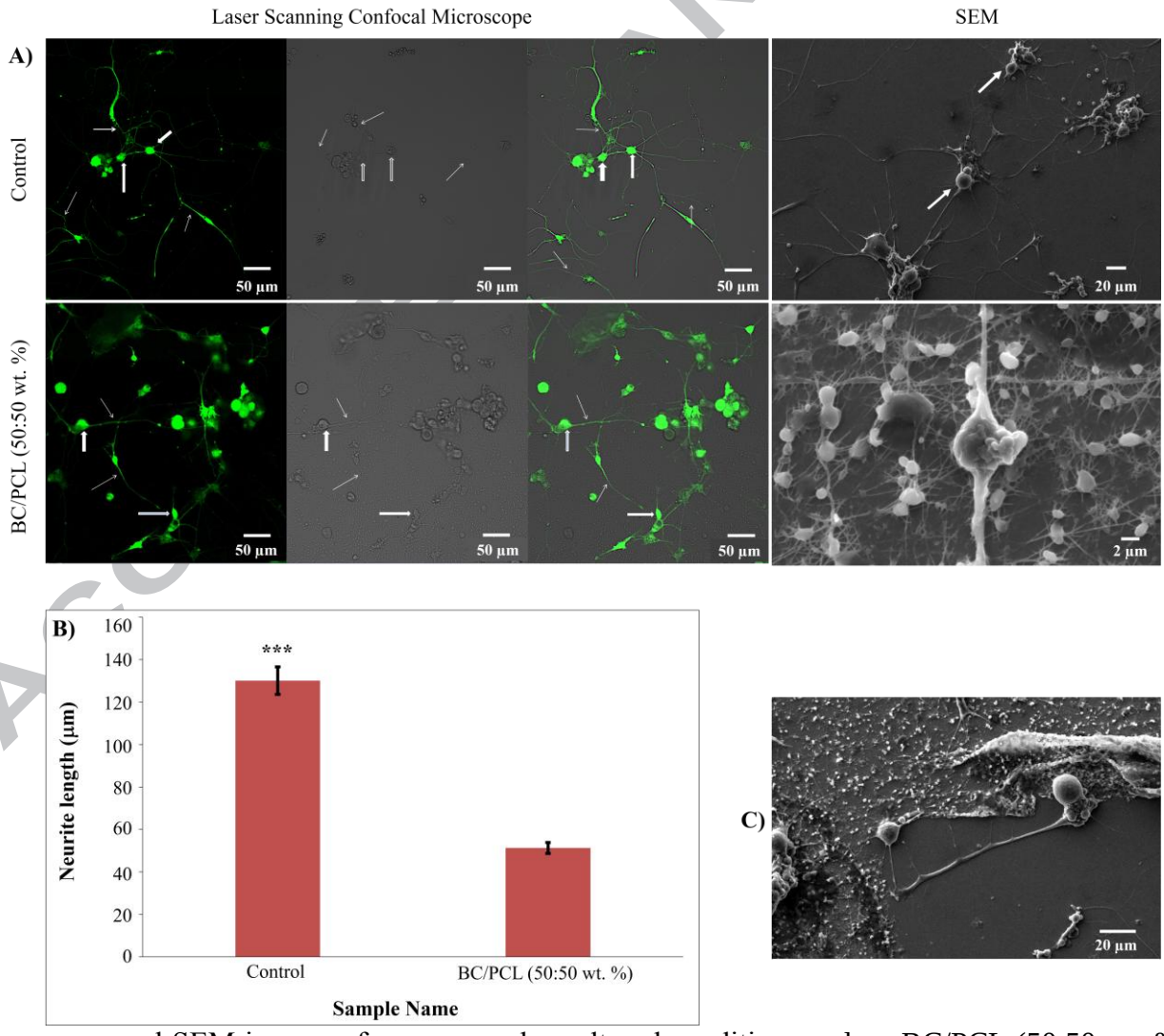

and axons, respectively). **B)** Axon size measurement chart indicating control and BC/PCL (50:50 wt. %) nanofibrous scaffold (p value <0.05 represented as ***). **C)** Extended neurites of DRG sensory neurons on BC/PCL (50:50 wt. %) nanofibrous scaffold.

To examine whether nanofibers influenced the extent of axonal growth, the lengths of all neurites were determined with Image J programme and are shown in **Figure 5B.** After 48 hours of incubation neurons on the BC/PCL (50:50 wt. %) nanofibrous scaffold had shorter axons compared to neurons on 5 wt. % PCL nanofibrous scaffold (51.3±6.9 and 130.1±7.5 μm, respectively, $p<0.05$). Stronger fasciculation of axons extending on 5 wt. % PCL nanofibrous scaffold may have caused the more intense growth on this substrate [74].

In SEM figure of BC/PCL (50:50 wt. %) nanofibrous scaffold (**Figure 5A**), neurite extensions appear, but it seems that extensions are buried in the scaffold, which is clear evidence indicating that the cells and sample have an interaction with each other. Besides, as can be seen on **Figure 5C**, the neurons on BC/PCL (50:50 wt. %) nanofibrous scaffolds were capable in extending their neurites to every region on the test slide to make synapses with other neurons even if there were no BC/PCL (50:50 wt. %) nanofiber. It can be explained as follows: if the BC/PCL (50:50 wt. %) nanofibrous scaffolds were used in human nervous system, new formed neurons on the BC/PCL (50:50 wt. %) nanofibrous scaffolds can provide neurite extensions and make connection with each other.

4. Conclusions

BC and PCL were successfully incorporated together to obtain firstly, BC/PCL (50:50 wt. %) blend solution and from it nanofibrous scaffolds by electrospinning. Obtained nanofibers were in the size scale 70-120 nm and embedded hollow micro/nanobeads spanned 100 nm–1.6 μm in size. Nanofibrous scaffold samples were characterized in terms of their crystallinity (FEG-SEM), ζ-potential and charge, FT-IR response, mechanical properties and biocompatibility. The structural features of the nanofibrous scaffolds closely mimic neurogical networks. The nanofibrous scaffolds produced in this study were not cytotoxic, they were biocompatible and promoted cell adhesion.

Moreover, experiments with DRG neurons used in primary cell culture showed that nearly all of the dorsal root ganglia were sticky and axon-extended and therefore compatible with BC/PCL (50:50 wt. %). The aligned BC/PCL (50:50 wt. %) nanofibers of the scaffold were highly supportive of the DRG cell culture and improved the neurite outgrowth. The ability of nanofibers to support orientated process elongation by both glia and neurons prompts further investigation into the possibility that such structures could form the basis for three-dimensional guidance scaffolds intended to promote nerve repair.

AUTHOR INFORMATION

Corresponding Author

***E-mail:** m.edirisinghe@ucl.ac.uk

Notes

The authors declare no competing financial interest.

Acknowledgements

The authors wish to thank UCL for part supporting of the electrospinning aspects of this work. The authors acknowledge the SurPASS™ 3 ζ-potential analyser support from Anton Paar GmbH, Graz, Austria. All animal procedures were approved by Medipol University Animal Experiments Ethics Committee (decision number is 38828770-604.01.01-E.46011) and all animal use and care were carried out in accordance with the European Community guidelines.

References

[1] T. Hudson, G. Evans, C. Schmidt, Engineering strategies for peripheral nerve repair, Orthop. Clin. North. Am. 31 (2000) 485- 498. https://doi.org/10.1016/S0030-5898(05)70166-8.

[2] F. Yang, R. Murugan, S. Ramakrishna, X. Wang, Y. X. Ma, S. Wang, Fabrication of nano-structured porous PLLA scaffold intended for nerve tissue engineering, Biomaterials 25 (2004) 1891-1900. https://doi.org/10.1016/j.biomaterials.2003.08.062.

[3] D. Gupta, J. Venugopal, M. P. Prabhakaran, V. R. G. Dev, S. Low, A. T. Choon, S. Ramakrishna, Aligned and random nanofibrous substrate for the in vitro culture of Schwann cells for neural tissue engineering, Acta. Biomater. 5 (2009) 2560-2569. https://doi.org/10.1016/j.actbio.2009.01.039.

[4] M. Ranjbar-Mohammadi, M. P. Prabhakaran, S. H. Bahrami, S. Ramakrishna, Gum tragacanth/poly(l-lactic acid) nanofibrous scaffolds for application in regeneration of peripheral nerve damage, Carbohydr. Polym. 140 (2016) 104-112. http://dx.doi.org/10.1016/j.carbpol.2015.12.012.

[5] W. Liu, S. Thomopoulos, Y. Xia, Electrospun nanofibers for regenerative medicine, Adv. Healthc. Mater. 1 (2012) 10-25. https://doi.org/10.1002/adhm.201100021.

[6] J. Wang, X. Yu, Preparation, characterization and in vitro analysis of novel structured nanofibrous scaffolds for bone tissue engineering, Acta. Biomater. 6 (2010) 3004-3012. https://doi.org/10.1016/j.actbio.2010.01.045.

[7] C. E. Schmidt, J. B. Leach, Neural tissue engineering: strategies for repair and regeneration, Annu. Rev. Biomed. Eng. 5 (2003) 293-347. https://doi.org/10.1146/annurev.bioeng.5.011303.120731.

[8] W. Zhu, C. O'Brien, J. B. O'Brien, L. G. Zhang, 3D nano/microfabrication techniques and nanobiomaterials for neural tissue regeneration, Nanomedicine 9 (2014) 859-875. https://doi.org/10.2217/nnm.14.36.

[9] Y. Li, Y. Xiao, C. Liu, The Horizon of Materiobiology: A Perspective on Material-Guided Cell Behaviors and Tissue Engineering, Chem. Rev. 117 (2017) 4376–4421. https://doi.org/10.1021/acs.chemrev.6b00654.

[10] S. A. Sell, P. S. Wolfe, K. Garg, J. M. McCool, I. A. Rodriguez, G. L. Bowlin, The Use of Natural Polymers in Tissue Engineering: A Focus on Electrospun Extracellular Matrix Analogues, Polymers 2 (2010) 522-553. https://doi.org/10.3390/polym2040522.

[11] M. Huang, Y. Si, X. Tang, Z. Zhu, B. Ding, L. Liu, G. Zheng, W. Luo, J. Yu, Gravity driven separation of emulsified oil–water mixtures utilizing in situ polymerized superhydrophobic and superoleophilic nanofibrous membranes, J. Mater. Chem. A 1 (2013) 14071-14074. https://doi.org/10.1039/c3ta13385k.

[12] Y. Si, T. Ren, B. Ding, J. Yu, G. Sun, Synthesis of mesoporous magnetic Fe_3O_4@carbon nanofibers utilizing in situ polymerized polybenzoxazine for water purification, J. Mater. Chem. 22 (2012) 4619-4622. https://doi.org/10.1039/C2JM00036A.

[13] J. M. Anderson, C. W. Patrick, A. G. Mikos, L. V. McIntire, Frontiers in Tissue Engineering, first ed., Pergamon, Oxford, 1988.

[14] R. C. Thomson, A. K. Shung, M. J. Yaszemski, A. G. Mikos, in Principles of Tissue Engineering, Vol. 2: R. Lanza, R. Langer, J. Vacanti (Eds), Academic Press, San Diego, USA 2000, pp. 61-251.

[15] A. R. Nectow, K. G. Marra, D. L. Kaplan, Biomaterials for the development of peripheral nerve guidance conduits, Tissue Eng. B Rev. 18 (2012) 40-50. https://doi.org/10.1089/ten.teb.2011.0240.

[16] M. Parhizkar, P. Sofokleous, E. Stride, M. Edirisinghe, Novel preparation of controlled porosity particle/fibre loaded scaffolds using a hybrid micro-fluidic and electrohydrodynamic technique, Biofabrication 6 (2014) 045010. https://doi.org/10.1088/1758-5082/6/4/045010.

[17] E. Donath, G. B. Sukhorukov, F. Caruso, S. A. Davis, H. Mohwald, Novel Hollow Polymer Shells by Colloid-Templated Assembly of Polyelectrolytes, Angew. Chem., Int. Ed. 37 (1998) 2201-2205. https://doi.org/10.1002/(SICI)1521-3773(19980904)37:16<2201::AID-ANIE2201>3.0.CO;2-E.

[18] H. Sah, R. Toddywala, Y. W. Chien, The influence of biodegradable microcapsule formulations on the controlled release of a protein, J. Control. Release 30 (1994) 201-211. https://doi.org/10.1016/0168-3659(94)90026-4.

[19] M. Cheng, J. Deng, F. Yang, Y. Gong, N. Zhao, X. Zhang, Study on physical properties and nerve cell affinity of composite films from chitosan and gelatin solutions, Biomaterials 24 (2003) 2871-2880. https://doi.org/10.1016/S0142-9612(03)00117-0.

[20] I. Vroman, L. Tighzert, Biodegradable Polymers, Materials 2 (2009) 307-344. https://doi.org/10.3390/ma2020307.

[21] C. H. Kim, M. S. Khil, H. Y. Kim, H. U. Lee, K. Y. Jahng, An improved hydrophilicity via electrospinning for enhanced cell attachment and proliferation, J. Biomed. Mater. Res. Part B Appl. Biomater. 78B (2006) 283-290. https://doi.org/10.1002/jbm.b.30484.

[22] W. J. Li, J. A. Cooper, R. L. Mauck, R. S. Tuan, Fabrication and characterization of six electrospun poly(alpha-hydroxy ester)-based fibrous scaffolds for tissue engineering applications, Acta Biomater. 2 (2006) 377-385. https://doi.org/10.1016/j.actbio.2006.02.005.

[23] F. Frattini, F. R. P. Lopes, F. M. Almeida, R. F. Rodrigues, L. C. Boldrini, M. A. Tomaz, A. F. Baptista, P. A. Melo, A. M. Martinez, Mesenchymal stem cells in a polycaprolactone conduit promote sciatic nerve regeneration and sensory neuron survival after nerve injury, Tissue Eng. A. 18 (2012) 2030-2039. https://doi.org/10.1089/ten.tea.2011.0496.

[24] Y. Qiu, L. Qiu, J. Cui, Q. Wei, Bacterial cellulose and bacterial cellulose-vaccarin membranes for wound healing, Mater. Sci. Eng. C. 59 (2016) 303-309. https://doi.org/10.1016/j.msec.2015.10.016.

[25] Y. J. Dahman, Nanostructured Biomaterials and Biocomposites from Bacterial Cellulose Nanofibers, Nanosci. Nanotechnol. 9 (2009) 5105-5122. https://doi.org/10.1166/jnn.2009.1466.

[26] D. W. Hutmacher, Scaffolds in tissue engineering bone and cartilage, Biomaterials 21 (2000) 2529-2543. https://doi.org/10.1016/S0142-9612(00)00121-6.

[27] N. Shah, M. Ul-Islam, W. A. Khattak, J. K. Park, Overview of bacterial cellulose composites: a multipurpose advanced material, Carbohydr. Polym. 98 (2013) 1585-1598. https://doi.org/10.1016/j.carbpol.2013.08.018.

[28] F. Kramer, D. Klemm, D. Schumann, N. Hessler, F. Wesar, W. Fried, D. Stadermann, Nanocellulose Polymer Composites as Innovative Pool for (Bio)Material Development, Macromol. Symp. 244 (2006) 136-148. https://doi.org/10.1002/masy.200651213.

[29] N. Petersen, P. Gatenholm, Bacterial cellulose-based materials and medical devices: current state and perspectives, Appl. Microbiol. Biotechnol. 91 (2011) 1277-1286. https://doi.org/10.1007/s00253-011-3432-y.

[30] S. W. P. Kemp, S. K. Walsh, R. Midha, Growth factor and stem cell enhanced conduits in peripheral nerve regeneration and repair, Neurol. Res. 30 (2008) 1030-1038. http://dx.doi.org/10.1179/174313208X362505.

[31] G. Monaco, R. Cholas, L. Salvatore, M. Madaghiele, A. Sannino, Sterilization of collagen scaffolds designed for peripheral nerve regeneration: Effect on microstructure, degradation and cellular colonization, Mater. Sci. Eng. 71 (2017) 335-344. https://doi.org/10.1016/j.msec.2016.10.030.

[32] J. Scheib, A. Höke, Advances in peripheral nerve regeneration, Nat. Rev. Neurol. 9 (2013) 668–676. https://doi.org/10.1038/nrneurol.2013.227.

[33] X. Hu, J. Huang, Z. Ye, L. Xia, M. Li, B. Lv, X. Shen, Z. Luo, A novel scaffold with longitudinally oriented microchannels promotes peripheral nerve regeneration, Tissue Eng. 15 (2009) 3297-3308. https://doi.org/10.1016/j.msec.2016.10.030.

[34] J. Huang, X. Hu, L. Lu, Z. Ye, Y. Wang, Z. Luo, Electrical stimulation accelerates motor functional recovery in autograft-repaired 10 mm femoral nerve gap in rats, J. Neurotrauma 10 (2009) 1805-1813. https://doi.org/10.1089/neu.2008.0732.

[35] L. Xu, S. Zhou, G. Y. Feng, L. P. Zhang, D. M. Zhao, Y. Sun, Q. Liu, F. Huang, Neural stem cells enhance nerve regeneration after sciatic nerve injury in rats, Mol. Neurobiol. 46 (2012) 265-274. https://doi.org/10.1007/s12035-012-8292-7.

[36] T. Maneerung, S. Tokura, R. Rujiravanit, Impregnation of silver nanoparticles into bacterial cellulose for antimicrobial wound dressing, Carbohydr. Polym. 72 (2008) 43-51. https://doi.org/10.1016/j.carbpol.2007.07.025.

[37] I. A. Sacui, R. C. Nieuwendaal, D. J. Burnett, S. J. Stranick, M. Jorfi, C. Weder, E. Foster, R. T. Olsson, J. W. Gilman, Comparison of the Properties of Cellulose Nanocrystals and Cellulose Nanofibrils Isolated from Bacteria, Tunicate, and Wood Processed Using Acid, Enzymatic, Mechanical, and Oxidative Methods, ACS Appl. Mater. Interfaces 6 (2014) 6127-6138. https://doi.org/10.1021/am500359f.

[38] R. T. Olsson, R. Kraemer, A. López-Rubio, S. Torres-Giner, M. J. Ocio, J. M. Lagarón, Extraction of Microfibrils from Bacterial Cellulose Networks for Electrospinning of Anisotropic Biohybrid Fiber Yarns, Macromolecules 43 (2010) 4201-4209. https://doi.org/10.1021/ma100217q.

[39] P. Paximada, E. A. Dimitrakopoulou, E. Tsouko, A. A. Koutinas, C. Fasseas, I. G. Mandala, Structural modification of bacterial cellulose fibrils under ultrasonic irradiation, Carbohydr. Polym. 150 (2016) 5-12. https://doi.org/10.1016/j.carbpol.2016.04.125.

[40] A. K. Singh, Engineered Nanoparticles: Structure, Properties and Mechanisms of Toxicity, first ed., Academic Press, Cambridge, 2015.

[41] O. Demir, N. Aysit, Z. Onder, N. Turkel, G. Ozturk, A. D. Sharrocks, I. A. Kurnaz, ETS-domain transcription factor Elk-1 mediates neuronal survival: SMN as a potential target, Bba-Mol. Basis Dis. 1812 (2011) 652-662. https://doi.org/10.1016/j.bbadis.2011.02.012.

[42] J. Lin, B. Ding, J. Yu, Direct Fabrication of Highly Nanoporous Polystyrene Fibers via Electrospinning, ACS Appl. Mater. Interfaces 2 (2010) 521–528. https://doi.org/0.1021/am900736h.

[43] Y. Liu, J.-H. He, J. Yu, H. Zeng, Controlling numbers and sizes of beads in electrospun nanofibers, Polym. Int. 57 (2008) 632–636. https://doi.org/10.1002/pi.2387.

[44] Q. P. Pham, U. Sharma, A. G. Mikos, Electrospinning of polymeric nanofibers for tissue engineering applications: a review, Tissue Eng. 12 (2006) 1197-1211. https://doi.org/10.1089/ten.2006.12.1197.

[45] H. L. Jiang, D. F. Fang, B. S. Hsiao, B. Chu, W. Chen, Optimization and characterization of dextran membranes prepared by electrospinning, Biomacromolecules 5 (2004) 326-333. https://doi.org/10.1021/bm034345w.

[46] H. Fong, I. Chun, D. H. Reneker, Beaded nanofibers formed during electrospinning, Polym. J. 40 (1999) 4585-4592. https://doi.org/10.1016/S0032-3861(99)00068-3.

[47] S. Zhu, H. Yu, Y. Chen, M. Zhu, Study on the Morphologies and Formational Mechanism of Poly(hydroxybutyrate-co-hydroxyvalerate) Ultrafine Fibers by Dry-Jet-Wet-Electrospinning, J. Nanomater. 2012 (2012) 1-8. https://doi.org/10.1155/2012/525419.

[48] J. Qian, Hollow Micro-/Nano-Particles from Biopolymers: Fabrication and Applications, ACS Symposium Series 1175 (2014) 257-287. https://doi.org/10.1021/bk-2014-1175.ch014.

[49] S. M. Marinakos, J. P. Novak, L. C. Brousseau, A. B. House, E. M. Edeki, J. C. Feldhaus, Gold Particles as Templates for the Synthesis of Hollow Polymer Capsules. Control of Capsule Dimensions and Guest Encapsulation, Am. Chem. Soc. 121 (1999) 8518-8522. https://doi.org/10.1021/ja990945k.

[50] N. Campbell, J. B. Reece, Nervous systems, in B. Wilbur (Ed.), Biology, Pearson Education Inc., San Francisco, 2002, p.1022.

[51] L. Ghasemi-Mobarakeh, M. Morshed, K. Karbalaie, M. A. Fesharaki, M. Nematallahi, M. H. Nasr-Esfahani, H. Baharvand, The thickness of electrospun poly (epsilon-caprolactone) nanofibrous scaffolds influences cell proliferation, Int. J. Artif. Organs 32 (2009) 150-158. https://doi.org/10.1177/039139880903200305.

[52] W. Yu, W. Zhao, C. Zhu, X. Zhang, D. Ye, W. Zhang, Y. Zhou, X. Jiang, Z. Zhang, Sciatic nerve regeneration in rats by a promising electrospun collagen/poly(ε-caprolactone) nerve conduit with tailored degradation rate, BMC Neurosci. 12 (2011) 1471-2202. https://doi.org/10.1186/1471-2202-12-68.

[53] M. S. Kim, G. H. Kim, Three-dimensional electrospun polycaprolactone (PCL)/alginate hybrid composite scaffolds, Carbohydr. Polym. 114 (2014) 213-221. https://doi.org/10.1016/j.carbpol.2014.08.008.

[54] A. Subramanian, U. M. Krishnan, S. Sethuraman, Development of biomaterial scaffold for nerve tissue engineering: Biomaterial mediated neural regeneration, J. Biomed. Sci. 16 (2009) 108-119. https://doi.org/10.1186/1423-0127-16-108.

[55] K. H. Lee, H. Y. Kim, M. S. Khil, Y. M. Ra, D. R. Lee, Characterization of nano-structured poly(ε-caprolactone) nonwoven mats via electrospinning, Polymer 44 (2003) 1287-1294. https://doi.org/10.1016/S0032-3861(02)00820-0.

[56] S. M. Lim, H. J. Lee, S. H. Oh, J. M. Kim, J. H. Lee, Novel fabrication of PCL porous beads for use as an injectable cell carrier system, J. Biomed. Mater. Res. Part B Appl. Biomater. 90 (2009) 521-530. https://doi.org/10.1002/jbm.b.31313.

[57] A. Mautner, K. Y. Lee, T. Tammelin, A. P. Mathew, A. J. Nedoma, K. Li, A. Bismarck, Cellulose nanopapers as tight aqueous ultra-filtration membranes, React. Funct. Polym. 86 (2015) 209-214. https://doi.org/10.1016/j.reactfunctpolym.2014.09.014.

[58] T. Luxbacher, The ZETA Guide – Principles of the streaming potential technique, Anton Paar GmbH, Graz, 2014.

[59] M. O. Aydogdu, E. Altun, M. Crabbe-Mann, F. Brako, F. Koc, G. Ozen, S. E. Kuruca, U. Edirisinghe, C. J. Luo, O. Gunduz, M. Edirisinghe, Cellular interactions with bacterial cellulose: Polycaprolactone nanofibrous scaffolds produced by a portable electrohydrodynamic gun for point-of-need wound dressing, Int. Wound. J. 15 (2018) 1-9. https://doi.org/10.1111/iwj.12929.

[60] M. O. Aydogdu, J. Chou, E. Altun, N. Ekren, S. Cakmak, M. Eroglu, A. A. Osman, O. Kutlu, E. T. Oner, G. Avsar, F. N. Oktar, I. Yilmaz, O. Gunduz, Production of the biomimetic small diameter blood vessels for cardiovascular tissue engineering, Int. J. Polym. Mater. (2018) 1-13. https://doi.org/10.1080/00914037.2018.1443930.

[61] V. Beachley, X. Wen, Polymer nanofibrous structures: Fabrication, biofunctionalization, and cell interactions, Prog. Polym. Sci. 35 (2010) 868-892. https://doi.org/10.1016/j.progpolymsci.2010.03.003.

[62] A. Finne-Wistrand, A. C. Albertsson, O. H. Kwon, N. Kawazoe, G. Chen, I. K. Kang, H. Hasuda, J. Gong, Y. Ito, Resorbable scaffolds from three different techniques: electrospun fabrics,

salt-leaching porous films, and smooth flat surfaces, Macromol. Biosci. 8 (2008) 951-959. https://doi.org/10.1002/mabi.200700328.

[63] P. Sangsanoh, S. Waleetorncheepsawat, O. Suwantong, P. Wutticharoenmongkol, O. Weeranantanapan, B. Chuenjitbuntaworn, P. Cheepsunthorn, P. Pavasant, P. Supaphol, In vitro biocompatibility of schwann cells on surfaces of biocompatible polymeric electrospun fibrous and solution-cast film scaffolds, Biomacromolecules 8 (2007) 1587-1594. https://doi.org/10.1021/bm061152a.

[64] Y. M. Chen, X. Tingfei, Y. Zheng, T. Guo, J. Hou, Y. Wan, Y. Gao, In Vitro Cytotoxicity of Bacterial Cellulose Scaffolds Used for Tissue-engineered Bone, J. Bioact. Compat. Polym. 24 (2009) 137-145. https://doi.org/10.1177/0883911509102710.

[65] R. Pértile, S. Moreira, F. Andrade, L. Domingues, M. Gama, Bacterial cellulose modified using recombinant proteins to improve neuronal and mesenchymal cell adhesion, Biotechnol. Prog. 28 (2012) 526-532. https://doi.org/10.1002/btpr.1501.

[66] L. Ghasemi-Mobarakeh, M. P. Prabhakaran, M. Morshed, M. H. Nasr-Esfahani, S. Ramakrishna, Electrospun poly(epsilon-caprolactone)/gelatin nanofibrous scaffolds for nerve tissue engineering, Biomaterials 29 (2008) 4532-4539. https://doi.org/10.1016/j.biomaterials.2008.08.007.

[67] Y. Z. Zhang, J. Venugopal, Z. M. Huang, C. T. Lim, S. Ramakrishna, Characterization of the surface biocompatibility of the electrospun PCL-collagen nanofibers using fibroblasts, Biomacromolecules 6 (2005) 2583-2589. https://doi.org/10.1021/bm050314k.

[68] C. J. Grande, F. G. Torres, C. M. Gomez, M. C. Bano, Nanocomposites of bacterial cellulose/hydroxyapatite for biomedical applications, Acta Biomater. 5 (2009) 1605-1615. https://doi.org/10.1016/j.actbio.2009.01.022.

[69] A. Svensson, E. Nicklasson, T. Harrah, B. Panilaitis, D. L. Kaplan, M. Brittberg, P. Gatenholm, Bacterial cellulose as a potential scaffold for tissue engineering of cartilage, Biomaterials 26 (2005) 419-431. https://doi.org/10.1016/j.biomaterials.2004.02.049.

[70] R. Pértile, S. Moreira, F. Andrade, L. Domingues, M. Gama, Bacterial cellulose modified using recombinant proteins to improve neuronal and mesenchymal cell adhesion, Biotechnol. Prog. 28 (2012) 526-532. https://doi.org/10.1002/btpr.1501.

[71] M. E. Barabas, E. C. Mattson, E. Aboualizadeh, C. J. Hirschmug, C. L. Stucky, Chemical structure and morphology of dorsal root ganglion neurons from naive and inflamed mice, J. Biol. Chem. 289 (2014) 34241-34249. https://doi.org/10.1074/jbc.M114.570101.

[72] A. Subramanian, U. M. Krishnan, S. Sethuraman, Fabrication of uniaxially aligned 3D electrospun scaffolds for neural regeneration, Biomed. Mater. 6 (2011) 1-10. https://doi.org/10.1088/1748-6041/6/2/025004.

[73] F. Yang, R. Murugan, S. Wang, S. Ramakrishna, Electrospinning of nano/micro scale poly(L-lactic acid) aligned fibers and their potential in neural tissue engineering, Biomaterials 26 (2005) 2603-2610. https://doi.org/10.1016/j.biomaterials.2004.06.051.

[74] E. Schnell, K. Klinkhammer, S. Balzer, G. Brook, D. Klee, P. Dalton, J. Mey, Guidance of glial cell migration and axonal growth on electrospun nanofibers of poly-epsilon-caprolactone and a collagen/poly-epsilon-caprolactone blend, Biomaterials 28 (2007) 3012-3025. https://doi.org/10.1016/j.biomaterials.2007.03.009.

ToC Information

Esra Altun, Mehmet O. Aydogdu, Sine O. Togay, Ahmet Z. Sengil, Nazmi Ekren, Merve E. Haskoylu, Ebru T. Oner, Nese A. Altuncu, Gurkan Ozturk, Maryam Crabbe-Mann, Jubair Ahmed, Oguzhan Gunduz and Mohan Edirisinghe*

Bioinspired Scaffold Induced Regeneration of Neural Tissue

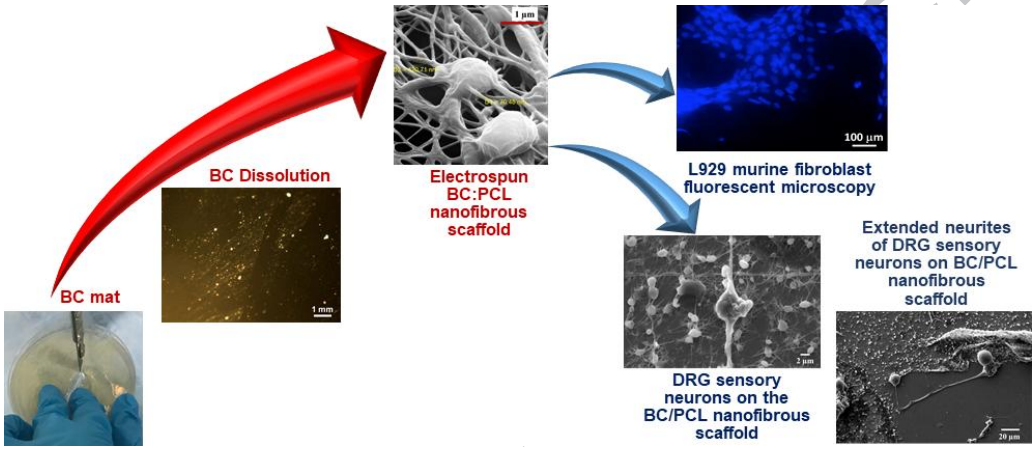

Highlights

- Nerve-like branched nanofibrous scaffolds were produced for nerve induced repair.
- Bacterial cellulose/Poly(ε-caprolactone) blend was used with electrospinning.
- The primary cell culture was performed using DRG cells on the scaffolds.
- Neural elongation and outgrowth followed the same direction as the nanofibers.
- The neurons on the scaffolds made synapses with other neurons to communicate.